J Musculoskelet Neuronal Interact 2013; 13(3):289-296

Original Article

Hylonome

Changes over time in structural plasticity of trabecular bone in rat tibiae immobilized by reversible sciatic denervation

H. Tamaki[1], K. Yotani[2], F. Ogita[2], H. Takahashi[1], H. Kirimto[1], H. Onishi[1], N. Yamamoto[1,3]

[1]Institute for Human Movement and Medical Sciences, Niigata University of Health and Welfare, 1398, Shimami, Kitaku, Niigata 950-3198, Japan; [2]National Institute of Fitness and Sports in Kanoya 1, Shiromizu, Kanoya, Kagoshima 891-2393, Japan; [3]Niigata Rehabilitation Hospital 761, Kisaki, Kitaku, Niigata 950-3304, Japan

Abstract

Objective: The present study aimed to clarify the structural recovery, and to compare the time course of morphological changes in trabeculae and the process of bone mass change in rat tibiae following temporary immobilization of hind limb by sciatic neurectomy or nerve freezing. **Methods:** In 11-week-old male Fischer 344 rats, 4-5 mm of the sciatic nerve was removed (neurectomy group) or frozen by 5-second application of a stainless steel rod immersed in liquid nitrogen (nerve-freezing group). Quantitative changes in cancellous bone were assessed by histomorphometry. **Results:** The results clarified that: trabecular bone volume (BV/TV) decreases until 3 weeks after denervation, and in the nerve-freezing group, it then increases from week 4, recovering to pre-surgery levels by week 10 (no recovery was seen in the neurectomy group); in the initial phase of bone atrophy, the decrease in BV/TV is more gradual in the nerve-freezing group than in the neurectomy group; and changes in trabecular architecture in the bone atrophy-recovery process are strongly associated with changes in trabecular thickness. **Conclusion:** The findings suggested that after transient injury by nerve freezing and subsequent recovery of neuromuscular function, bone tissue undergoes recovery from bone loss, but that trabeculae may not show complete structural recovery.

Keywords: Disuse, Recovery, Trabecular Morphology, Atrophy, Injury

Introduction

The mass and structure of bone tissue adapt to the mechanical loading of gravity and movement. Limb disuse due to denervation causes musculoskeletal atrophy, together with a large reduction in bone mass and changes in trabecular architecture[1-4]. Bone strength is determined by bone mass, quality and structure, with trabecular architecture being a contributing factor[5,6]. Disused bone exhibits loss of mass through reduced bone formation and increased bone resorption[2,7,8]. Some findings have suggested that thinning and fragmentation of trabeculae are involved in the disappearance of cancellous bone when there is a decrease in mechanical factors through disuse or deficits in endocrine factors due to procedures such as ovariectomy[9]. Trabecular fragmentation involves disruption of the mechanically effective crisscross structure, and there is thought to be a marked disappearance of trabeculae at sites of reduced transmission of mechanical stimulus[9]. Decreased bone mass due to reduced mechanical loading or decreases in humoral factors related to bone metabolism is reversible; the use of pharmaceuticals or exercise training to promote bone formation or suppress bone resorption improves mineralization and increases bone mass through increased thickness of the cortical bone or trabeculae[10,11]. However, it is also thought that once trabeculae are severed, reconnection is unlikely to occur[12]. Even when bone mass recovers after temporary disuse bone atrophy, it is unclear whether the trabecular architecture completely recovers[13].

Nerve-freezing methods can be used to immobilize innervated muscles by paralyzing nerve function for certain periods, thus creating a disuse model of temporary damage that also al-

The authors have no conflict of interest.

Corresponding author: Hiroyuki Tamaki, Ph.D., Institute for Human Movement and Medical Sciences, Niigata University of Health and Welfare, 1398, Shimami, Kitaku, Niigata 950-3198, Japan
E-mail: hiroyuki-tamaki@nuhw.ac.jp

Edited by: D. Burr
Accepted 7 May 2013

	0 w	1 w	2 w	3 w	4 w	5 w	10 w
Cont	217±14	244±17	263±23	279±18*	290±17*	299±15*	342±19*
NF	225±14	233±13	254±23	271±12*	274±21*	289±23*	339±21*
SN	220±17	230±14	244±14	267±15*	273±14*	282±13*	324±22*

Table 1. Body weight (g) of control (Cont), sciatic nerve freezing (NF) and neurectomized (SN) rat groups in each time point after surgery. Values are means ± SD. *P<0.05 vs. basal controls.

lows experimental observation of the post-atrophy recovery process[14-16]. We have previously reported functional and structural recovery of skeletal muscle in 3-4 weeks using this model.

Based on these earlier studies, we hypothesized that after transient injury by nerve freezing and subsequent recovery of neuromuscular function following recovery, bone tissue follows a process of recovery from atrophy in terms of mass, but that trabeculae may not show complete structural recovery. There was also uncertainty about the extent of bone mass decrease and subsequent recovery time following nerve freezing, and so a comparison with a neurectomy-induced disuse model was necessary.

The present study aimed to clarify these uncertainties by using histomorphometric methods to compare the time course of morphological changes in trabeculae, and the process of bone mass change, in rat tibiae following temporary immobilization of hind leg by sciatic neurectomy and nerve freezing. We also investigated the structural plasticity of trabeculae over time during recovery from bone atrophy induced by transient injury-induced disuse.

Materials and methods

Animals and denervation

Experimental animals were 104 11-week-old male Fischer 344 rats (weight during experiment: 217-343 g, Table 1) kept in a controlled environment of 23±2ºC, 55±5% humidity and a 12-hour light, 12-hour dark lighting cycle. Rats were maintained on a diet of rodent chow (CE-2; CLEA Japan, Tokyo, Japan) and given water *ad libitum*. All procedures were performed in accordance with the guidelines presented in the Guiding Principles for the Care and Use of Animals in the Field of Physiological Sciences, published by the Physiological Society of Japan. This study was approved by the Animal Committee of the National Institute of Fitness and Sports (#21-1).

Before surgery, animals were anaesthetized by intraperitoneal injection of sodium pentobarbitone (50 mg/kg). The skin covering the buttock was incised and the left sciatic nerve was exposed and separated from the surrounding tissue. The sciatic nerve was supported from below using tweezers, and in the neurectomy group (SN, n=36 total, n=6 at each time point, body weight, 228±15 g), 4-5 mm of the nerve was removed, whereas in the nerve freezing group (NF, n=36 total, n=6 at each time point, body weight, 225±12 g), the exposed sciatic nerve was frozen by 5-second application of a stainless steel rod (diameter 3 mm) frozen in liquid nitrogen at -180ºC[14,16]. This freezing procedure was selected as the method of denervation as it uniformly damages nerve fibers, although reinnervation is more likely to occur with this technique than using other procedures, such as nerve crushing, cutting or transecting with a suture[14,16-18]. As age-matched experimental controls, 24 rats were subjected to sham surgeries in which the sciatic nerve was exteriorized but not removed (sham control, n=4 at each time point, body weight, 217±14 g). The incision was then closed with sutures and each animal was kept in a standard cage[15]. Tibiae were collected from the SN and NF groups before surgery (basal control, n=8, body weight, 223±14 g) and at 1, 2, 3, 4, 5 and 10 weeks after surgery, together with those from the sham operation group. Before histochemical analysis, the length of each tibia was measured three times along the bone's long axis using vernier calipers accurate to 0.01 mm, and the median value was taken as data.

Bone histomorphometry

Experimental rats were anaesthetized with sodium pentobarbitone (50 mg/kg body weight), mixed fixative (1% glutaraldehyde, 1% formaldehyde and 0.05% $CaCl_2$ dissolved in 0.1 mol/L sodium cacodylate buffer, pH 7.35) was injected via the abdominal aorta and perfusion fixation was allowed to occur at room temperature for 30 minutes. For paraffin-embedded block preparation, each tibia was cut sagittally at the proximal end and immersed in the same fixative for a further 90 minutes[11]. Samples were decalcified in 0.1 mol/L EDTA for 4-6 weeks at 4°C. These were then dehydrated in a graded ethanol series, cleared with xylene and embedded in paraffin. Using a microtome, longitudinal sections (5 μm) per block were created from the paraffin-embedded blocks. Specimens were stained with hematoxylin and eosin (H-E), Azan or toluidine blue. H-E staining according to the Goland-Yoshiki method[19,20] was used to stain osteoid in the decalcified specimens. First, bone tissue that had been dehydrated in a graded ethanol series was immersed for two days in a solution of cyanuric chloride. Specimens were then cleared in ethanol and decalcified in EDTA at 4°C. The embedded paraffin blocks were then sliced and stained with hematoxylin and eosin B.

For frozen carboxymethyl cellulose (CMC) gel block preparation reported by Kawamoto & Shimizu[21], after perfusion fixation above mentioned, samples for use as undecalcified specimens were first frozen temporarily in isopentane cooled using liquid nitrogen. Samples were then prepared according

to a previously reported method[22,23].

Standard bone histomorphometric nomenclature, symbols and units were used as described in the report of the American Society for Bone and Mineral Research Histomorphometry Nomenclature Committee[24]. Bone histomorphometric analysis was performed at a minimum of eight optic fields with 100-fold magnification[25] using a light/fluorescence microscope (BX50; Olympus, Tokyo, Japan) with a semiautomatic image analyzing system (Bone Histomorphometry, System Supply Co, Nagano, Japan)[26-28]. Histomorphometric analysis was performed in the secondary spongiosa in the metaphysis of the proximal tibiae, not including the primary spongiosa located under the growth plate. An image of the specimen was processed using a semiautomatic image analyzing system to measure the primary parameters: bone area (BV, μm^2), tissue area (TV, μm^2) and bone surface (BS, μm). From these primary parameters, the following parameters were calculated: bone volume (BV/TV, %), trabecular thickness (Tb.Th, μm) and trabecular separation (Tb.Sp, μm). More than 15 separate regions for calculating mean osteoid thickness (O. Th) were measured per field at 400-fold magnification[26] using image analysis software (Image-Pro Plus 5; Media Cybernetics, Rockville, MD, USA)[29].

Statistical analysis

All data are expressed as means ± standard deviation. Kruskal-Wallis test followed by the Dunn's multiple test was used to compare experimental groups at each time point with control groups. Pearson's correlation coefficient was used to determine the relationship between per-week percentage change in BV/TV (ΔBV/TV) and per-week percentage changes in trabecular architecture parameters (ΔTb.Th, ΔTb.Sp). Significance levels were set at $P<0.05$.

Results

Rats subjected to neurectomy (SN) and nerve freezing (NF) were able to flex their hip joints, but dragged their feet on the denervated side when moving. The ankle and toe were also completely immobile when the animals were suspended by their tails for testing the lower limb movement, and in the SN group, this remained the case throughout the experiment. In the first week after denervation, NF rats began exhibiting air stepping using their legs when subjected to tail suspension test. By the third week, movement and support accompanied by voluntary dorsiflexion of the foot were possible, and subsequently, animals were able to move around their cages with no signs of paralysis. During the experimental period there was no inhibition of longitudinal bone growth; the tibiae of NF and SN animals steadily increased in mean length from 31.2 mm to 41.3 mm. Neither were there any significant differences between groups from week to week, or in comparison with the control group (Figure 1).

Morphological changes in the metaphyseal secondary spongiosa of proximal tibiae resulting from SN and NF began to appear in the first week after denervation. Trabecular bone volume (BV/TV) decreased rapidly by 37-49% in week 1, and

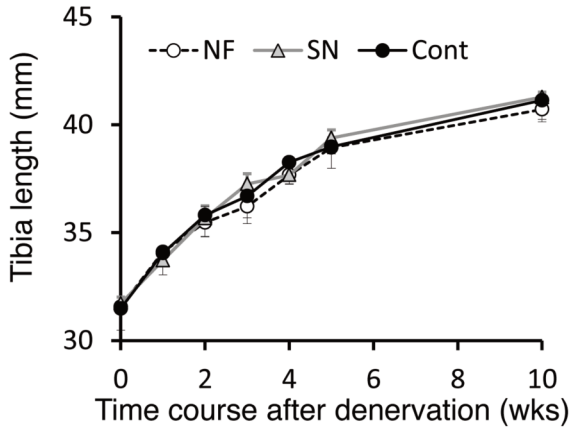

Figure 1. Time course of tibia length of control, sciatic nerve freezing and neurectomized legs. ○Cont; sham control, ▲NF; nerve freezing, ■SN; sciatic neurectomy. Values are means ± SD.

subsequently, a steadily slowing disappearance of trabeculae was observed (Figure 2A). When compared with the SN group, the rate of BV/TV decrease in the initial period after denervation was slower in NF, and there was a significant difference ($P<0.05$) between groups in week 2. In week 3, however, BV/TV in SN and NF had fallen to the same level. The SN group showed no changes in BV/TV from week 3 after denervation, but the NF group showed a gradual increase from week 4, increasing to 52% of pre-surgery levels in week 5 and 99% in week 10, reaching a level not significantly different from the basal control. The results of trabecular architecture analysis showed that in the NF group, Tb.Th were significantly lower than in the control group from 1 week after denervation ($P<0.05$) (Figure 2). Tb.Th in the NF group steadily decreased until week 3, then began increasing from week 4 onwards, and in week 5 had recovered to the extent that it no longer differed significantly from the control group value (Figure 2B). In the SN group, Tb.Th and Tb.Sp continued to steadily decrease up to week 10 after denervation without showing any recovery.

Figure 3 shows light micrographs of trabecular tissue from the metaphyseal secondary spongiosa of proximal tibiae at week 5 after denervation, when trabecular thickness in the NF group had recovered to a level not significantly different from control group levels. H-E stain (Yoshiki's method) produces deep red staining of only the unmineralized collagen matrix of osteoid. Observations of the location of osteoid and osteoblasts revealed that in the NF group, the osteoid traversed the length of the trabecular strut with osteoblasts lining its outer edge (Figure 3C). Furthermore, where there are two separate trabecular struts along the same line, the space between the termini of the separated trabeculae contained no osteoblasts, and no osteoid layer was visible (Figure 3D). In the SN group, osteoid width was narrower than in NF and the gaps between trabecular termini contained no osteoblasts and no osteoid layer (Figure 3E, F). In contrast, in the control group there was ev-

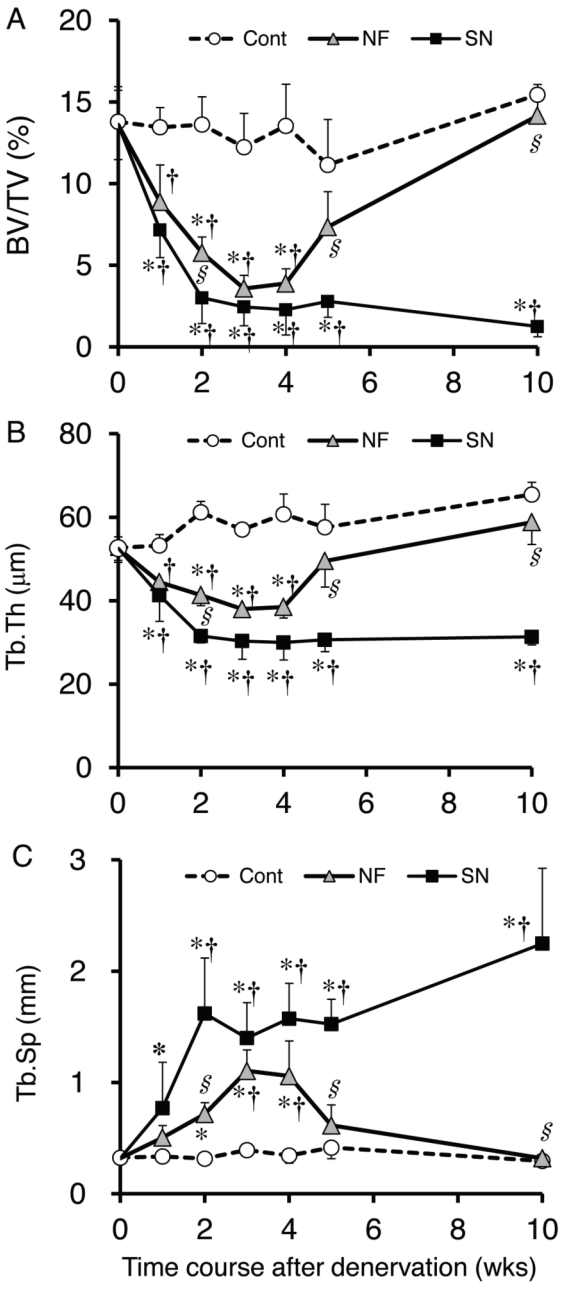

Figure 2. Time course of trabecular bone volume (BV/TV; %) and structural parameters (**A-C**) in the proximal tibial metaphysis of control, sciatic nerve freezing and neurectomized legs. ○Cont; sham control, ▲NF; nerve freezing, ■SN; sciatic neurectomy. *P<0.05 vs. basal controls. §P<0.05 vs. Cont. #P<0.05 vs. SN. Values are means ± SD.

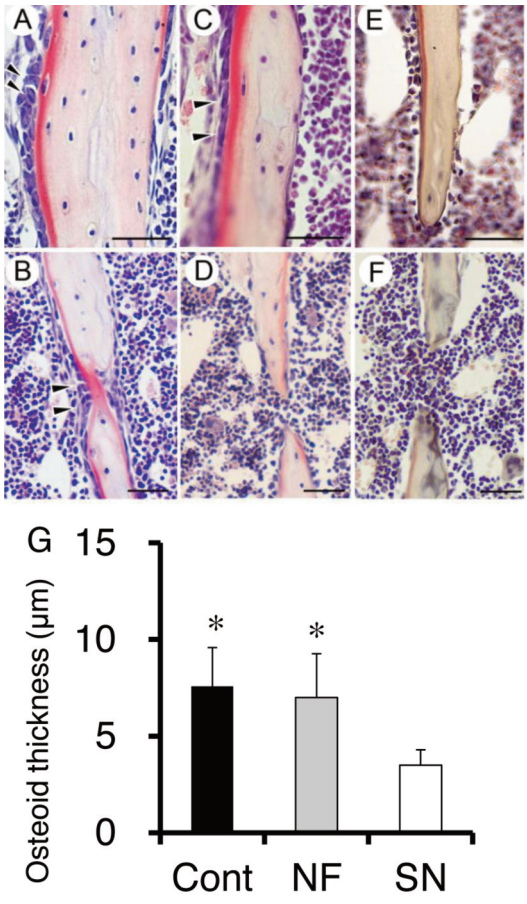

Figure 3. Light micrographs show distinct eosinophilia of osteoid matrix at the trabecular bone stained with hematoxylin and eosin (**A-F**) and quantitative histomorphometric analysis for mean osteoid thickness (**G**) at 5 weeks after denervation. Osteoid matrix is lined with osteoblasts (arrow head). Bar=50 μm. A-B; sham control, C-D; nerve freezing, E-F; neurectomy.

idence of osteoid formation: osteoid width was thicker than in the NF and SN groups and osteoblasts had accumulated in the space between trabecular termini (Figure 3A, B). Osteoid thickness in the NF group was significantly greater than in the SN group (P<0.05) and did not differ significantly from the control group (Figure 3G).

The correlation was analyzed between percentage change in trabecular bone volume (ΔBV/TV) and the three factors of ΔTb.Th and ΔTb.Sp from the post-denervation atrophy phase through the recovery phase (Figure 4). A significant correlation was observed between ΔBV/TV and ΔTb.Th (P<0.001), which had the highest correlation coefficient at 0.95. On multiple regression analysis to identify the factors in trabecular architecture influencing ΔBV/TV, the standard partial regression coefficient for ΔTb.Th was significantly higher than for ΔTb.Sp (P<0.05) (Table 2).

Discussion

Our study clarified the following: 1) BV/TV decreases until 3 weeks after denervation. Subsequently, in NF, it steadily increases from week 4 and recovers to pre-surgery levels by week 10. However, in SN it does not recover. 2) Changes in trabecular architecture in the bone loss-recovery process are strongly associated with changes in trabecular thickness.

Firstly, we should discuss the different effects of the SN and

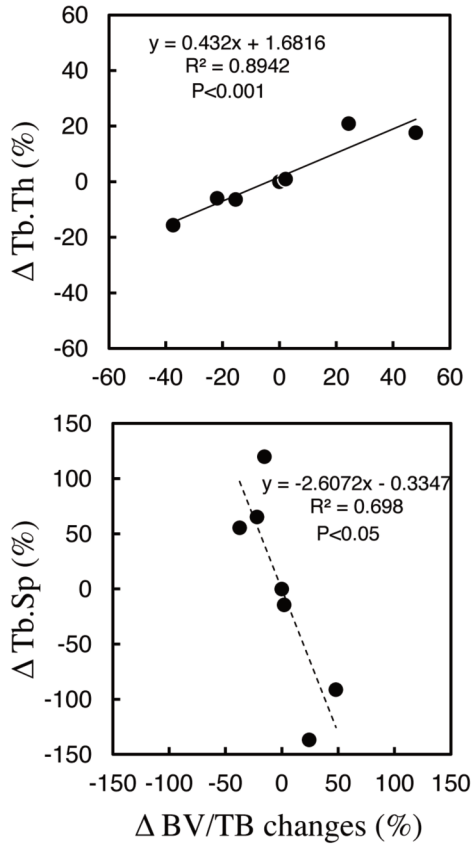

Figure 4. Correlations between percent changes in trabecular bone volume (ΔBV/TV) and structural parameters (Δtrabecular thickness; ΔTb.Th, Δtrabecular separation; ΔTb.Sp).

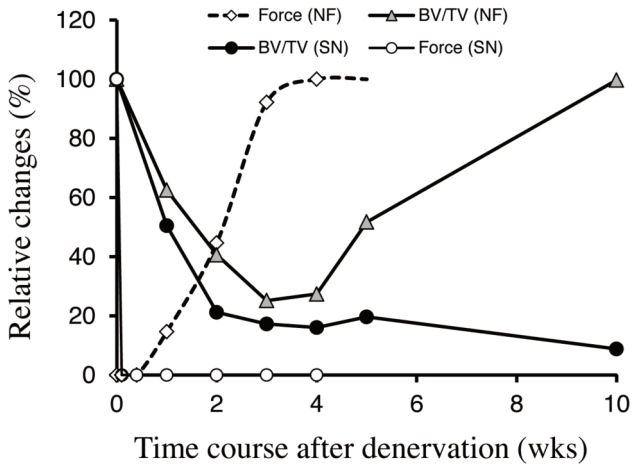

Figure 5. Relative changes to the basal control in trabecular bone volume and muscle force after sciatic neurectomy (SN) and nerve freezing (NF). Data on muscle force are cited from Takekura et al.[16] and Nishizawa et al.[17].

NF procedures. SN creates a long lasting leg disuse model for situations where subsequent natural recovery is undesired. In contrast, NF creates a temporary disuse model that allows complete immobilization of the innervated muscles for a certain period by temporarily disabling peripheral nerve function, thus allowing observation of the post-atrophy recovery process. In a previous study investigating the neuromuscular function recovery process after sciatic nerve freezing[16], twitch force in the soleus muscle and extensor digitorum longus muscle induced by electrical stimulation of the sciatic nerve was completely absent until day 3 after NF, and then slowly began to recover in the first week, and by week 3, had recovered to pre-NF levels, and to the force levels with direct muscle stimulation. With regard to leg movement in this study, knee flexion was seen at the first week after NF, supportive movement of the hind leg on the denervated side was seen during locomotor movement at around 3 weeks after NF. These findings were absent in SN animals[30]. In our previous study observing synaptic microarchitecture[17], parameters including the nerve terminal area and synaptic vesicle density began slowly recovering at 1 week after NF, and by week 4 there was also structural recovery to basal control levels. In this study, we compared changes in cancellous bone area in the NF group and the SN group. The bone loss process showed a gentle decrease in the NF group, but there were no significant differences at week 3, when the lowest BV/TV levels were reached. Subsequently, bone mass in the NF group steadily increased from week 4, recovering to a level not significantly different from basal controls by week 10. The SN group showed no increases in BV/TV during the experimental period. These results suggest that the nerve freezing method is also applicable to bone tissue as a method for observing the consecutive processes of atrophy and recovery after temporary functional denervation and subsequent reinnervation. In addition to the factor of mechanical loading, neuromuscular injury related factors or neurotransmitters could also influence bone remodeling. Bone is highly innervated by sensory and sympathetic nerves and contains neuromediators[31-33]. Denervation of sensory and sympathetic nerves has been shown to affect bone remodeling[34,35]. It would be interesting to clarify the fate of specific populations of nerve fibers that innervate the bone following the neuromuscular injury, disuse and recovery process, as secretion of a neurotrophic or growth factor and neurotransmitters would be a more directly plausible mechanism affecting bone remodeling after denervation[36-39].

Secondly, with regard to the BV/TV recovery process after NF, investigation of the plastic changes in trabecular architecture revealed that from 3 weeks after NF, BV/TV steadily increased, reaching a level at 5 weeks that was significantly higher than the lowest level at 3 weeks, and recovering to about 50% of basal control. Looking at the recovery of neuromuscular function from the perspective of muscle twitch force, recovery to 50% of basal control levels occurred at about 2 weeks[16], thus suggesting a time lag of about 3 weeks between the 50% recovery time of muscle and that of bone tissue (Figure 5). It would therefore be necessary to consider the recovery levels of different tissues when implementing exercise therapy

Correlation coefficient		
	Tb.Th	Tb.Sp
BV/TV (%)	0.945	-0.835
(P value)	0.001	0.019
Standard partial regression coefficient		
	Tb.Th	Tb.Sp
BV/TV (%)	1.057	0.123
(P value)	0.049	0.763

Table 2. Correlation coefficients and standard partial regression coefficient between percent changes in trabecular bone volume and structural parameters.

during the recovery period. With regard to the time course of changes in trabecular architecture during the recovery process after NF, increases in Tb.Th were correlated with increases in BV/TV, which suggests that increased trabecular thickness contributes more to cancellous bone recovery.

We found that: 1) the correlation coefficient for ΔBV/TV and ΔTb.Th was higher; 2) the standard partial regression coefficient for ΔTb.Th was also significantly higher. Trabecular bone volume and thickness have also been found to show a significantly higher correlation (r=0.763) in age-related bone loss[40]. These results show that changes in trabecular thickness in the post-NF bone loss and recovery phases have the larger impact on trabecular bone volume, and suggest that trabecular thickness possesses structural plasticity.

At 5 weeks, when BV/TV and trabecular thickness had significantly recovered, osteoid thickness was significantly higher in NF than SN, and was about the same as in controls (Figure 4). This suggests that bone collagen formation by osteoblasts in NF had recovered to a higher level than in SN. Observation of sites of osteoid formation further revealed that where two separated trabecular struts were present along the same line, osteoid formation and osteoblasts were abundant along the length of the trabecular struts, but the gap between the fractured trabecular termini contained no osteoid layer and no osteoblasts (Figure 3D, F). Therefore, the main function of the enhanced osteoid formation seen in the recovery period in the NF group appears to increase trabecular thickness. This finding may also indicate that osteoid does not readily form along the long axis of trabeculae in such a way as to connect fragmented trabeculae. It is also speculated that once severed, reconnection between trabeculae does not readily occur[12], and that even if trabeculae recover their mass, complete structural recovery is not achieved.

Limitation

Our study had several limitations. The first relates to our use of bone morphometry based on 2-dimensional histomorphometry, which has long been considered the gold standard. However, a 2D design has limits when trying to understand a 3-dimensional structure. In a comparison of trabecular architecture using both methods studied in rat tibiae, good correlation was obtained between both techniques[41]. 3D μCT methods is a valid technique for bone mass and micro-architecture measurements in rat model of disuse osteoporosis[42]. Furthermore, the limited histomorphometric parameters were reported in the present study. Further information on the other histomorphometric data would increase understanding of bone loss-recovery process.

The second limitation was that, like many of the reported studies, we performed kinematic checks on the contralateral leg but did not quantify the activity levels of the experimental animals during the experiment. Unlike Kingery et al.[43], we did not measure locomotor activity or quantify weight bearing. However, in our previous study[16], we quantified the muscle strength recovery process. In the future, an evaluation of the amount of daily activity in experimental animals, together with biomechanical data would be of greater use in understanding disuse osteopenia.

Conclusion

In this study, we observed the features of morphological changes and the time course of trabecular bone loss in tibiae after temporary leg immobilization by sciatic neurectomy and nerve freezing. We also compared the structural plasticity of trabecular bone in the subsequent recovery process. Morphological changes in trabecular bone due to SN and NF began in the first week after surgery: trabecular bone volume showed a gradual decrease up to week 3 (2.5% and 3.8% in BV/TV, respectively), but the extent of decrease was less pronounced in NF. In the process of recovery of trabecular bone volume after NF, recovery to about 50% of the basal control level was achieved by week 5, and to 96% by week 10 (7.9% and 14.2% in BV/TV, respectively). Changes in trabecular thickness were the factor most strongly associated with percentage change in trabecular bone volume. In the process of trabecular bone recovery from disuse after temporary denervation and subsequent reinnervation, trabecular thickness was the only structural feature to show recovery.

Acknowledgements

This work was supported in part by a Grant-in-Aid for Scientific Research from the Japan Society for the Promotion of Science (C, project nos. 18200512 and 22500611), and by a Grant-in-Aid for Developed Research (B) from the Niigata University of Health and Welfare. The authors are grateful to the Niigata Bone Science Institute for the technical support in histomorphometry.

References

1. Turner RT, Bell NH. The effects of immobilization on bone histomorphometry in rats. J Bone Miner Res 1986; 1:399-407.
2. Wakley GK, Baum BL, Hannon KS, Turner RT. The effects of tamoxifen on the osteopenia induced by sciatic

neurotomy in the rat: a histomorphometric study. Calcif Tissue Int 1988;43:383-8.
3. Wronski TJ, Morey ER. Inhibition of cortical and trabecular bone formation in the long bones of immobilized monkeys. Clin Orthop Relat Res 1983:269-76.
4. Young DR, Niklowitz WJ, Brown RJ, Jee WS. Immobilization-associated osteoporosis in primates. Bone 1986; 7:109-17.
5. Ito M, Ohki M, Hayashi K, Yamada M, Uetani M, Nakamura T. Relationship of spinal fracture to bone density, textural, and anthropometric parameters. Calcif Tissue Int 1997;60:240-4.
6. Jensen KS, Mosekilde L, Mosekilde L. A model of vertebral trabecular bone architecture and its mechanical properties. Bone 1990;11:417-23.
7. Weinreb M, Rodan GA, Thompson DD. Osteopenia in the immobilized rat hind limb is associated with increased bone resorption and decreased bone formation. Bone 1989;10:187-94.
8. Zeng QQ, Jee WS, Bigornia AE, King JG Jr, D'Souza SM, Li XJ, Ma YF, Wechter WJ. Time responses of cancellous and cortical bones to sciatic neurectomy in growing female rats. Bone 1996;19:13-21.
9. Yoshida S, Yamamuro T, Okumura H, Takahashi H. Microstructural changes of osteopenic trabeculae in the rat. Bone 1991;12:185-94.
10. Kannus P, Sievanen H, Jarvinen TL, Jarvinen M, Kvist M, Oja P, Vuori I, Jozsa L. Effects of free mobilization and low- to high-intensity treadmill running on the immobilization-induced bone loss in rats. J Bone Miner Res 1994;9:1613-9.
11. Tamaki H, Akamine T, Goshi N, Kurata H, Sakou T. Effects of exercise training and etidronate treatment on bone mineral density and trabecular bone in ovariectomized rats. Bone 1998;23:147-53.
12. Bourrin S, Palle S, Genty C, Alexandre C. Physical exercise during remobilization restores a normal bone trabecular network after tail suspension-induced osteopenia in young rats. J Bone Miner Res 1995;10:820-8.
13. Maeda H, Kimmel DB, Raab DM, Lane NE. Musculoskeletal recovery following hindlimb immobilization in adult female rats. Bone 1993;14:153-9.
14. Sakakima H, Kawamata S, Kai S, Ozawa J, Matsuura N. Effects of short-term denervation and subsequent reinnervation on motor endplates and the soleus muscle in the rat. Arch Histol Cytol 2000;63:495-506.
15. Takekura H, Kasuga N, Kitada K, Yoshioka T. Morphological changes in the triads and sarcoplasmic reticulum of rat slow and fast muscle fibres following denervation and immobilization. J Muscle Res Cell Motil 1996; 17:391-400.
16. Takekura H, Tamaki H, Nishizawa T, Kasuga N. Plasticity of the transverse tubules following denervation and subsequent reinnervation in rat slow and fast muscle fibres. J Muscle Res Cell Motil 2003;24:439-51.
17. Nishizawa T, Yamashia S, McGrath KF, Tamaki H, Kasuga N, Takekura H. Plasticity of neuromuscular junction architectures in rat slow and fast muscle fibers following temporary denervation and reinnervation processes. J Muscle Res Cell Motil 2006;27:607-15.
18. Tomori K, Ohta Y, Nishizawa T, Tamaki H, Takekura H. Low-intensity electrical stimulation ameliorates disruption of transverse tubules and neuromuscular junctional architecture in denervated rat skeletal muscle fibers. J Muscle Res Cell Motil 2010;31:195-205.
19. Yoshiki S. A simple histological method for identification of osteoid matrix in decalcified bone. Stain Technol 1973;48:233-8.
20. Yoshiki S, Toda H, Chiba I. Further considerations on a simple histological method for identification of osteoid matrix. Stain Technol 1974;49:367-73.
21. Kawamoto T, Shimizu M. A method for preparing 2- to 50-micron-thick fresh-frozen sections of large samples and undecalcified hard tissues. Histochem Cell Biol 2000;113:331-9.
22. Yuki A, Yotani K, Tamaki H, Kasuga N, Takekura H. Upregulation of osteogenic factors induced by high-impact jumping suppresses adipogenesis in marrow but not adipogenic transcription factors in rat tibiae. Eur J Appl Physiol 2010;109:641-50.
23. Tamaki H, Murata F, Takekura H. Histomorphological evidence of muscle tissue damage and recording area using coiled and straight intramuscular wire electrodes. Eur J Appl Physiol 2006;98:323-7.
24. Parfitt AM, Drezner MK, Glorieux FH, Kanis JA, Malluche H, Meunier PJ, Ott SM, Recker RR. Bone histomorphometry: standardization of nomenclature, symbols, and units. Report of the ASBMR Histomorphometry Nomenclature Committee. J Bone Miner Res 1987; 2:595-610.
25. Takahashi M, Yukata K, Matsui Y, Abbaspour A, Takata S, Yasui N. Bisphosphonate modulates morphological and mechanical properties in distraction osteogenesis through inhibition of bone resorption. Bone 2006;39:573-81.
26. Fujimoto R, Tanizawa T, Nishida S, Yamamoto N, Soshi S, Endo N, Takahashi HE. Local effects of transforming growth factor-beta1 on rat calvaria: changes depending on the dose and the injection site. J Bone Miner Metab 1999;17:11-7.
27. Hoshino K, Hanyu T, Arai K, Takahashi HE. Mineral density and histomorphometric assessment of bone changes in the proximal tibia early after induction of type II collagen-induced arthritis in growing and mature rats. J Bone Miner Metab 2001;19:76-83.
28. Sugimoto M, Futaki N, Harada M, Kaku S. Effects of combined treatment with eldecalcitol and alendronate on bone mass, mechanical properties, and bone histomorphometry in ovariectomized rats: a comparison with alfacalcidol and alendronate. Bone 2013;52:181-8.
29. Huang TH, Muhlbauer RC, Tang CH, Chen HI, Chang GL, Huang YW, Lai YT, Lin HS, Yang WT, Yang RS. Onion decreases the ovariectomy-induced osteopenia in

young adult rats. Bone 2008;42:1154-63.
30. Tamaki H, Yotani K, Yuki A, Nishizawa T, Tomori K, Kirimoto H, Ogita F, Takekura H. Alterations in trabecular bone architecture and muscle atrophy following sciatic neurectomy in rat tibiae. J Bone Miner Res 2009; 24:S250-1.
31. Mach DB, Rogers SD, Sabino MC, Luger NM, Schwei MJ, Pomonis JD, Keyser CP, Clohisy DR, Adams DJ, O'Leary P, Mantyh PW. Origins of skeletal pain: sensory and sympathetic innervation of the mouse femur. Neuroscience 2002;113:155-66.
32. Burt-Pichat B, Lafage-Proust MH, Duboeuf F, Laroche N, Itzstein C, Vico L, Delmas PD, Chenu C. Dramatic decrease of innervation density in bone after ovariectomy. Endocrinology 2005;146:503-10.
33. Castaneda-Corral G, Jimenez-Andrade JM, Bloom AP, Taylor RN, Mantyh WG, Kaczmarska MJ, Ghilardi JR, Mantyh PW. The majority of myelinated and unmyelinated sensory nerve fibers that innervate bone express the tropomyosin receptor kinase A. Neuroscience 2011; 178:196-207.
34. Hill EL, Turner R, Elde R. Effects of neonatal sympathectomy and capsaicin treatment on bone remodeling in rats. Neuroscience 1991;44:747-55.
35. Cherruau M, Facchinetti P, Baroukh B, Saffar JL. Chemical sympathectomy impairs bone resorption in rats: a role for the sympathetic system on bone metabolism. Bone 1999;25:545-51.
36. Itzstein C, Espinosa L, Delmas PD, Chenu C. Specific antagonists of NMDA receptors prevent osteoclast sealing zone formation required for bone resorption. Biochem Biophys Res Commun 2000;268:201-9.
37. Togari A, Arai M. Pharmacological topics of bone metabolism: the physiological function of the sympathetic nervous system in modulating bone resorption. J Pharmacol Sci 2008;106:542-6.
38. Bonnet N, Pierroz DD, Ferrari SL. Adrenergic control of bone remodeling and its implications for the treatment of osteoporosis. J Musculoskelet Neuronal Interact 2008; 8:94-104.
39. Ding Y, Arai M, Kondo H, Togari A. Effects of capsaicin-induced sensory denervation on bone metabolism in adult rats. Bone 2010;46:1591-6.
40. Weinstein RS, Hutson MS. Decreased trabecular width and increased trabecular spacing contribute to bone loss with aging. Bone 1987;8:137-42.
41. David V, Laroche N, Boudignon B, Lafage-Proust MH, Alexandre C, Ruegsegger P, Vico L. Noninvasive *in vivo* monitoring of bone architecture alterations in hindlimb-unloaded female rats using novel three-dimensional microcomputed tomography. J Bone Miner Res 2003; 18:1622-31.
42. Barou O, Valentin D, Vico L, Tirode C, Barbier A, Alexandre C, Lafage-Proust MH. High-resolution three-dimensional micro-computed tomography detects bone loss and changes in trabecular architecture early: comparison with DEXA and bone histomorphometry in a rat model of disuse osteoporosis. Invest Radiol 2002;37:40-6.
43. Kingery WS, Offley SC, Guo TZ, Davies MF, Clark JD, Jacobs CR. A substance P receptor (NK1) antagonist enhances the widespread osteoporotic effects of sciatic nerve section. Bone 2003;33:927-36.